Changes in contractile activation characteristics of rat fast and slow skeletal muscle fibres during regeneration

Paul Gregorevic, David R. Plant, Nicole Stupka and Gordon S. Lynch

Department of Physiology, The University of Melbourne, Victoria 3010, Australia

Damaged skeletal muscle fibres are replaced with new contractile units via muscle regeneration. Regenerating muscle fibres synthesize functionally distinct isoforms of contractile and regulatory proteins but little is known of their functional properties during the regeneration process. An advantage of utilizing single muscle fibre preparations is that assessment of their function is based on the overall characteristics of the contractile apparatus and regulatory system and as such, these preparations are sensitive in revealing not only coarse, but also subtle functional differences between muscle fibres. We examined the Ca^{2+}- and Sr^{2+}-activated contractile characteristics of permeabilized fibres from rat fast-twitch (extensor digitorum longus) and slow-twitch (soleus) muscles at 7, 14 and 21 days following myotoxic injury, to test the hypothesis that fibres from regenerating fast and slow muscles have different functional characteristics to fibres from uninjured muscles. Regenerating muscle fibres had ∼10% of the maximal force producing capacity (P_o) of control (uninjured) fibres, and an altered sensitivity to Ca^{2+} and Sr^{2+} at 7 days post-injury. Increased force production and a shift in Ca^{2+} sensitivity consistent with fibre maturation were observed during regeneration such that P_o was restored to 36–45% of that in control fibres by 21 days, and sensitivity to Ca^{2+} and Sr^{2+} was similar to that of control (uninjured) fibres. The findings support the hypothesis that regenerating muscle fibres have different contractile activation characteristics compared with mature fibres, and that they adopt properties of mature fast- or slow-twitch muscle fibres in a progressive manner as the regeneration process is completed.

(Resubmitted 8 April 2004; accepted after revision 1 June 2004; first published online 4 June 2004)
Corresponding author G. S. Lynch: Department of Physiology, The University of Melbourne, Victoria 3010, Australia. Email: gsl@unimelb.edu.au

As a biological motor, a skeletal muscle fibre is defined by its capacity to generate and sustain force and to change length. Evolution has conferred upon mammalian skeletal muscle the mechanisms with which to synthesize isoforms of critical contractile and regulatory proteins (Bottinelli & Reggiani, 2000). The diversity in contractile and regulatory protein isoform expression means that muscle fibres can exhibit unique contractile characteristics optimized to the functional requirements of individual muscles (Lynch *et al.* 1995; Bottinelli & Reggiani, 2000; Pette & Staron, 2000).

The functional capacity of a muscle is impaired when its fibres are injured (Rosenblatt, 1992). To restore functionality, the damaged units must be replaced with new fibres via muscle regeneration (Carlson & Faulkner, 1983). Postnatal synthesis of muscle fibres begins with the activation of otherwise quiescent satellite cells that reside within muscles. In response to muscle injury, satellite cells proliferate and differentiate to generate a population of myoblasts committed to muscle fibre formation. Ensuing myoblast alignment and serial fusion produces an elongated myotube, which during maturation develops the cytoskeletal and contractile filament architecture of a muscle fibre (Carlson & Faulkner, 1983; Donovan & Faulkner, 1987; Carlson *et al.* 2001).

Over the course of muscle regeneration, maturing muscle fibres are composed of different isoforms of contractile and regulatory proteins (Marechal *et al.* 1984; d'Albis *et al.* 1988; Whalen *et al.* 1990; Cantini *et al.* 1993; Noirez *et al.* 2000; Pette *et al.* 2002; Fink *et al.* 2004); however, little is known of the functional characteristics of individual muscle fibres during the earliest stages of regeneration. Therefore, we chose to examine the contractile activation characteristics of single fibres isolated from mammalian skeletal muscles during the early events of muscle regeneration. Considerable information regarding the contractile phenotype of a muscle fibre can be obtained not only by its myofibrillar ATPase activity and maximum velocity of shortening but also by

 DOI: 10.1113/jphysiol.2004.066217

characteristics associated with the process of activation by Ca^{2+}, such as the sensitivity to Ca^{2+}, the force per cross-sectional area, and the degree of cooperativity in development of Ca^{2+}-activated force (Bortolotto *et al.* 2000). Furthermore, when Sr^{2+} replaces Ca^{2+} as the activating ion, skeletal muscle fibres display quite striking differences with respect to the relationship between $[Ca^{2+}]$ or $[Sr^{2+}]$ and force production, i.e. their force–pCa and force–pSr relations. The force–pCa (–pSr) data represent the overall characteristics of the contractile apparatus and regulatory system and are sensitive in revealing not only coarse but also subtle functional differences between fibres (Lynch *et al.* 1995). Type I (slow-twitch) and type II (fast-twitch) fibres exhibit differential sensitivity to Sr^{2+}, facilitating identification of discrete fibre classes (Lynch *et al.* 1995). Type II fibres are characterized by relatively steep force–pCa (–pSr) relations and a large difference in their relative sensitivity to Ca^{2+} and Sr^{2+} ($pCa_{50} - pSr_{50} > 1.0$). Type I fibres are distinguished by their relatively shallow force–pCa (–pSr) relations and their smaller differential sensitivity to Ca^{2+} and Sr^{2+} ($pCa_{50} - pSr_{50} < 0.5$) (see Lynch *et al.* 1995).

Some evidence suggests that during muscle regeneration there may be a bias in the formation of specific fibre types, where the contractile and regulatory protein isoform composition of a regenerating muscle fibre is influenced by the source of satellite cells (Feldman & Stockdale, 1991; Canti-ni *et al.* 1993; Rosenblatt *et al.* 1996; Erzen *et al.* 1999; Martelly *et al.* 2000). However, many stimuli contribute to regulation of protein expression within skeletal muscle fibres *in vivo* (Snoj-Cvetko *et al.* 1996; Pette & Staron, 2000). Whether regenerating fibres from fast-twitch or slow-twitch muscles exhibit similar contractile activation characteristics during the early stages of development is unclear.

We examined the contractile characteristics of permeabilized fibres from regenerating fast-twitch and slow-twitch muscles at various time points following myotoxic injury. We tested the hypothesis that regenerating muscle fibres from the rat fast-twitch extensor digitorum longus and slow-twitch soleus muscles exhibit atypical contractile characteristics initially, but as regeneration progresses these properties become increasingly fibre type specific.

Methods

All procedures were approved by the Animal Experimentation Ethics Committee of The University of Melbourne and conformed to the Guidelines for the Care and Use of Experimental Animals described by the National Health and Medical Research Council of Australia. Adult 6-month-old male Fischer 344 rats (400–450 g) were housed in groups of four under an artificial light–dark cycle and provided with unlimited access to drinking water and standard chow for the duration of the experiments.

Experimental muscle injury

Intramuscular injection of bupivacaine to a muscle's holding capacity causes complete destruction of all muscle fibres whereas non-muscle cells remain unaffected (Rosenblatt, 1992; Carlson & Faulkner, 1996; Carlson *et al.* 2001). Muscle regeneration commences during the days immediately post-injection such that in rat muscles, myoblasts are evident by 4 days post-injury, and full functional recovery is achieved within 60 days (Rosenblatt, 1992; Rosenblatt & Woods, 1992). The nature of the bupivacaine injury model makes it an effective tool for simulating muscle injury and studying muscle regeneration independent of the complications associated with vascular and nerve damage commonly observed with other models of injury such as crush (Hurme *et al.* 1991; Noonan *et al.* 1994).

The rats were anaesthetized with methohexitone sodium (Brietal, Eli Lilly, IN, USA, 60 mg (kg body mass)$^{-1}$ I.P.) such that they were unresponsive to tactile stimuli. The extensor digitorum longus (EDL) and soleus muscles of the right hindlimb were surgically exposed and each muscle injected with a maximal volume of ~800–1000 μl of 0.5% bupivacaine hydrochloride (Marcain, Astra, North Ryde, NSW, Australia). This was equivalent to, or exceeded, the maximum injection volume capacity for limb muscles of this mass, and caused degeneration of all muscle fibres (Gregorevic *et al.* 2002). Following injection, the small skin incision was closed (Michel clips, Aesculap, Tuttlingen, Germany). Rats were returned to their cages upon regaining full consciousness, where they remained until killing at 7, 14 or 21 days post-injury. There were no obvious impairments in walking or weight bearing in the animals and they moved about their cages freely upon waking. Rats were examined daily to ensure health and general condition. The time points were selected in order to examine myotubes as early in formation as possible, and at intervals corresponding to progressive (albeit incomplete) fibre maturation and growth (Rosenblatt & Woods, 1992; Devor & Faulkner, 1999).

At the time of kill, rats were anaesthetized with pentobarbital sodium (60 mg (kg body mass)$^{-1}$ I.P.) to a depth of anaesthesia that prevented all responses to tactile stimuli. Once an appropriate depth of anaesthesia had been

attained, the rats were killed by cardiac excision. Injured and uninjured EDL and soleus muscles were surgically excised from the right and left hindlimbs, respectively. The muscles were blotted once on filter paper and tied at the proximal and distal tendons to glass capillary tubes at a taut length. The muscles were immersed in a permeabilizing (chemical skinning) solution (mM, except where noted: glycerol, 50% v/v; potassium propionate, 125; imidazole, 20; EGTA, 5; ATP, 2; $MgCl_2$, 2, pH 7.1) and stored at −20°C for not more than 4 months.

Single muscle fibre isolation and measurement of contractile activation characteristics

On the day of testing, individual muscles were removed from storage and placed in a Petri dish containing ice-chilled skinning solution, where permeabilized fibre segments were carefully separated from the muscle bundle using fine forceps with the aid of a dissecting microscope. One end of each muscle fibre segment was tied with braided surgical silk (10–0, Deknatel, New York, NY, USA) to a pin affixed directly to a sensitive force transducer (AE801, SensorOne Technologies Corporation, Sausalito, CA, USA), and the other end of the fibre was clamped between the jaws of a fixed pair of jewellers' forceps (no. 5, A. Dumont & Fils, Switzerland). Following mounting, fibre segment length and diameter were estimated using a calibrated reticle mounted in the eyepiece of a microscope. Sarcomere length (estimated from He–Ne laser diffraction maxima along the length of the fibre segment) was adjusted to 2.7 μm, which is within the optimal range for force generation by mammalian muscle fibres (Stephenson & Williams, 1982).

The contractile activation characteristics of each fibre were evaluated by manipulating the fibre bathing solutions as previously described (Lynch *et al.* 1995; Plant & Lynch, 2002; Lamb & Posterino, 2003). Fibres were initially incubated in a relaxing solution (mM: K^+, 125; Hepes, 60; EGTA, 50; Na^+, 36; creatine phosphate, 10; Mg^{2+}, 10.3; ATP, 8; NaN_3, 1), rinsed in a wash solution (equivalent composition except for equimolar HDTA in place of EGTA) and then incubated in increasing concentrations of Ca^{2+}- and then Sr^{2+}-buffered solutions ($7.16 \leq \mathrm{pCa} \leq 4.68$, and $5.5 \leq \mathrm{pSr} \leq 3.69$, respectively, where $\mathrm{pCa} = -\log_{10}[Ca^{2+}]$ ($\mathrm{pSr} = -\log_{10}[Sr^{2+}]$). The Ca^{2+} activating solution contained 50 mM added Ca^{2+} (pCa ∼4.68]). The Sr^{2+} activating solution contained 40 mM SrEGTA and 10 mM $EGTA^{2-}$. All solutions contained 1 mM free $[Mg^{2+}]$, ionic strength ∼154 mM with pH adjusted to 7.10 ± 0.05 with KOH. The K_{app} values of Ca^{2+} and Sr^{2+} to EGTA at pH 7.10 and in the presence of 1 mM Mg^{2+} were determined previously to be 4.78×10^6 M^{-1} and 1.91×10^4 M^{-1}, respectively (Fink *et al.* 1986). All experiments were performed at 22 ± 1°C. All activating solutions were stored for later potentiometric titrations in order determine the exact pCa of each solution (Moisescu & Thieleczek, 1978).

Force−pCa and force−pSr characteristics were determined for each fibre using the well established protocols that have been described in detail previously (Lynch *et al.* 1995; Bortolotto *et al.* 2000). Maximum Ca^{2+}-activated force (P_o) was normalized for the estimated fibre cross-sectional area, based on fibre diameter measurements that assumed a circular cross-section (sP_o, kN m^{-2}).

To define parameters that described the relationship between force and $[Ca^{2+}]$ or $[Sr^{2+}]$, the percentage of the maximum Ca^{2+} (or Sr^{2+})-activated force developed by a fibre in various activating solutions had to be calculated. This was done by dividing the steady-state isometric force attained in a solution of a particular pCa or pSr by the interpolated value of the maximum Ca^{2+}- or Sr^{2+}-activated force response. The force produced at each pCa (pSr) was expressed as a percentage of the maximum Ca^{2+} (Sr^{2+})- activated force in that fibre. Plots of force *versus* pCa (pSr) for each fibre were fitted with Hill curves by the analysis program GraphPad Prism (GraphPad Software Inc., San Diego, CA, USA) to obtain the slope and the pCa_{50} (pSr_{50}), i.e. the pCa (pSr) value giving half-maximum force (see Bortolotto *et al.* 2000). A Hill equation was used to plot the experimental data for individual fibres against a curve for the theoretical ideal force−pCa (−pSr) relationship, where (for Ca^{2+}) relative force $(P_r) = K[Ca^{2+}]^{n_{Ca}}/(1 + K[Ca^{2+}]^{n_{Ca}})$, where K is a constant related to pCa_{50} by the expression $\log_{10}K = n_{Ca}pCa_{50}$. Force−pCa (−pSr) relations were used to determine the threshold for contractile activation (pCa_{10}, pSr_{10}) and the fibre sensitivity to the activating ions (pCa_{50}, pSr_{50}). Preliminary analysis indicated no differences in Ca^{2+}- and Sr^{2+}-activated contractile characteristics between fibres from the uninjured (contralateral) limb and those from normal sedentary (cage control) rats. Therefore, a separate group of cage control rats (involving no bupivacaine-induced injury) was not deemed necessary.

Determination of myosin heavy chain isoform composition in regenerating skeletal muscles

Myosin heavy chain (MyHC) isoform composition was determined in whole muscle homogenates using sodium

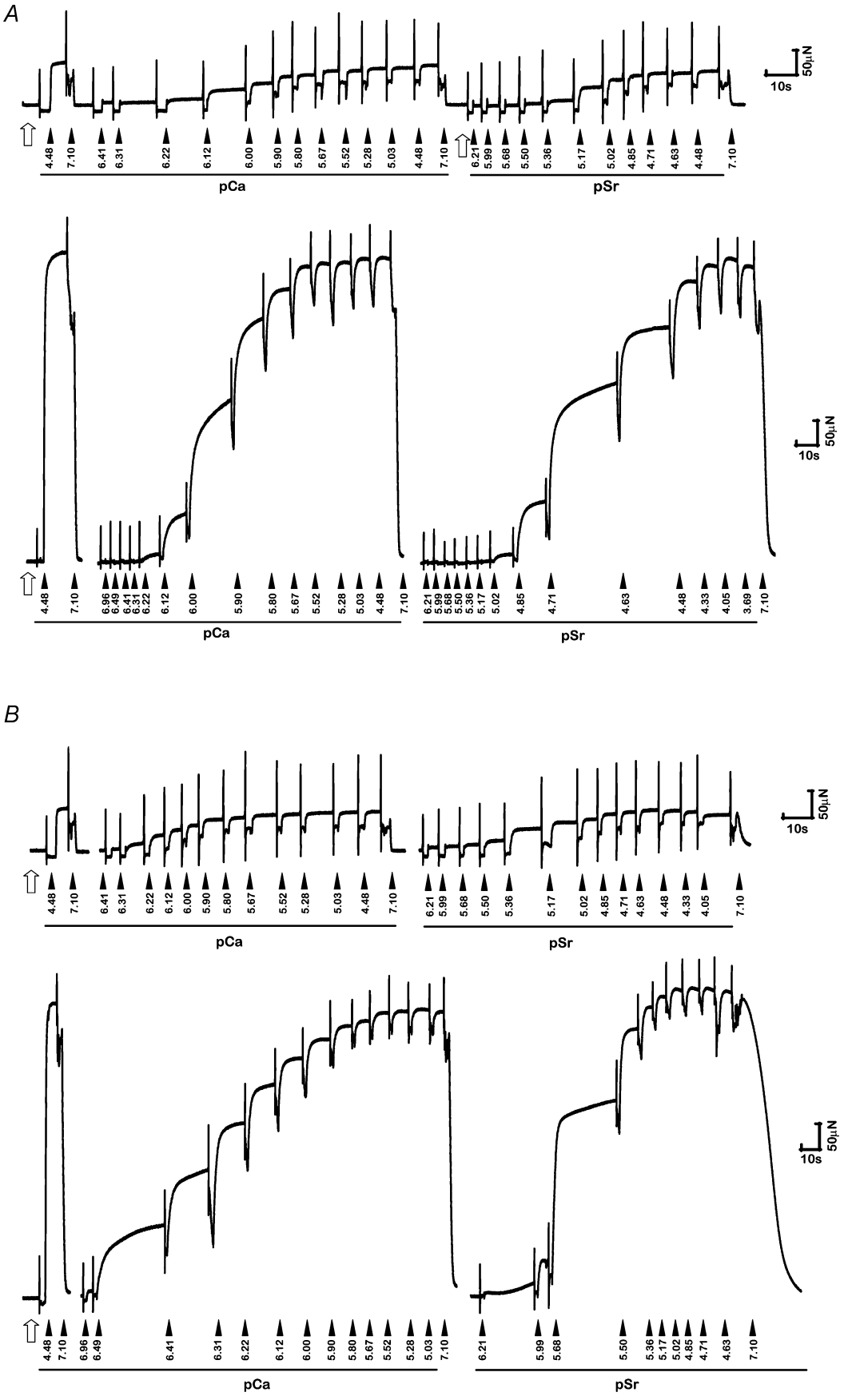

dodecyl sulphate–polyacrylamide gel electrophoresis (SDS-PAGE) based on techniques previously described (Talmadge & Roy, 1993) except that 0.08% β-mercaptoethanol was added to the upper and lower running buffer to improve MyHC isoform resolution, and proteins were visualized using a commercially available silver stain kit (no. LC6100, InVitrogen Corporation, Melbourne, Australia). Gels were run and analysed in duplicate. The region of gels containing the MyHC isoforms were scanned and a computerized image analysis system was used to determine the proportion of each MyHC isoform (Talmadge & Roy, 1993). MyHC isoforms were identified based on the separation criteria described by Bigard *et al.* (1996, 2001), Pette *et al.* (2002), and Fink *et al.* (2004).

Statistics

All values in the text, figures, and tables are reported as means ± S.E.M. unless indicated otherwise. Data for contractile activation characteristics of single fibres from EDL and soleus muscles were compared across time points (uninjured, 7, 14 and 21 days post-injury) using a general linear model, two factor analysis of variance (ANOVA) and Fisher's LSD *post hoc* multiple comparison procedure to identify differences between specific groups of fibres. In all cases, differences between groups were considered significant when $P < 0.05$.

Results

The results described here summarize data obtained from the examination of different muscle fibre segments sampled from uninjured and injured EDL and soleus muscles of 20 rats, sampled 7, 14 and 21 days (d) following myotoxic injury. The number of fibres sampled for each time point is listed in the tables.

The Ca^{2+}- and Sr^{2+}-activated contractile characteristics (including values for pCa_{50}, pSr_{50}, n_{Ca}, n_{Sr}, $pCa_{50} - pSr_{50}$) of fibres from uninjured (contralateral) muscles were consistent with those we have published previously from muscles of similarly aged sedentary cage control rats (Lynch *et al.* 1995; Plant & Lynch, 2001). Raw force traces showing Ca^{2+} and Sr^{2+} activation of isolated permeabilized fibres from injured and uninjured EDL and soleus muscles are presented in Fig. 1.

Seven days post-injury

At 7 days post-injury (the earliest time point of examination after myotoxic injury), fibres from regenerating EDL muscles ($n = 19$) were less than 10% the cross-sectional area of fibres sampled from uninjured muscles ($n = 30$) of the contralateral limb (7 d EDL fibres, injured: $308 \pm 59\ \mu m^2$ *versus* $4015 \pm 327\ \mu m^2$, Table 1). P_o of regenerating EDL muscle fibres at 7 d (0.06 ± 0.01 mN) was ∼10% that for uninjured EDL muscle fibres. The sP_o values for the 7 d EDL fibres were variable although they averaged over 300 kN m^{-2}, a reflection on the ability of these very small regenerating fibres to produce forces (normalized to fibre cross-sectional area) that were similar to or even higher than fibres from uninjured muscles. In 7 d EDL fibres the threshold for activation occurred at lower $[Ca^{2+}]$ and $[Sr^{2+}]$ as indicated by the higher pCa_{10} and pSr_{10} values. Similarly, fibre sensitivity to Ca^{2+} and Sr^{2+} was increased, with pCa_{50} and pSr_{50} obtained at ∼40% and ∼62% lower free cation concentrations, respectively (Table 1). In addition, the differential sensitivity ($pCa_{50} - pSr_{50}$) of 7 d EDL fibres was ∼16% lower than uninjured EDL muscle fibres, indicating that regenerating EDL muscle fibres were more sensitive to both Ca^{2+} and Sr^{2+} than uninjured fibres (see Fig. 2*A*). The Hill coefficients (n_{Ca} and n_{Sr}) for 7 d EDL fibres were reduced ∼37% and 28%, respectively, compared with uninjured EDL muscle fibres, indicating that the normally steep force−pCa (−pSr) relations were shallow, and more characteristic of those for control (uninjured) type I (slow) muscle fibres.

Similar to the regenerating EDL muscle fibres examined at 7 days post-injury, fibres from regenerating soleus

Figure 1. Raw force traces showing Ca^{2+} and Sr^{2+} activation of isolated permeabilized fibres
Raw force traces showing Ca^{2+} and Sr^{2+} activation of isolated permeabilized fibres from EDL (*A*) and soleus (*B*) muscles of the rat at 7 days post-injury (upper panel in each case) and from uninjured muscles (lower panel in each case). Note the obvious differences in absolute force producing capacity between injured/regenerating and uninjured fibres. Filled arrowheads indicate the sequential transfer of an isolated fibre segment into solutions of differing $[Ca^{2+}]$ (or $[Sr^{2+}]$). The numbers accompanying each arrow refer to the estimated pCa or pSr in each case. The open arrow indicates fibre is bathed in pre-activating (low-relaxing) solution. For each activation sequence, a fibre was always transferred from relaxing solution to pre-activation solution and incubated for 1 min before being transferred into activating solutions of differing $[Ca^{2+}]$ and $[Sr^{2+}]$.

Table 1. Summary of data for permeabilized muscle fibres from uninjured and regenerating rat EDL muscles examined 7, 14 and 21 days after myotoxic injury

	Control ($n = 30$)	7d ($n = 19$)	14d ($n = 21$)	21d ($n = 17$)
CSA (μm^2)	4015 ± 327	308 ± 59*	1400 ± 99*	2079 ± 224*
P_o (mN)	0.67 ± 0.05	0.06 ± 0.01*	0.23 ± 0.02*	0.30 ± 0.03*
sP_o (kN m^{-2})	178 ± 10	332 ± 51*	173 ± 12	166 ± 16
pCa_{10}	6.15 ± 0.02	6.46 ± 0.02*	6.29 ± 0.03*	6.26 ± 0.03*
pCa_{50}	6.00 ± 0.01	6.21 ± 0.02*	6.09 ± 0.03*	6.06 ± 0.03
n_{Ca}	6.26 ± 0.33	4.00 ± 0.20*	5.16 ± 0.09*	4.57 ± 0.20*
pSr_{10}	4.94 ± 0.02	5.47 ± 0.03*	5.16 ± 0.03*	5.07 ± 0.04*
pSr_{50}	4.73 ± 0.02	5.14 ± 0.01*	4.92 ± 0.02*	4.83 ± 0.03*
n_{Sr}	4.91 ± 0.20	3.06 ± 0.17*	4.27 ± 0.31*	4.05 ± 0.09*
$pCa_{50} - pSr_{50}$	1.27 ± 0.01	1.07 ± 0.01*	1.17 ± 0.02*	1.23 ± 0.01

Values are means ± S.E.M.; *n*, no. of fibres; CSA, estimated fibre cross-sectional area; P_o, maximum isometric force; sP_o, specific P_o; pCa_{10}, $[Ca^{2+}]$ required for 10% maximal activation (threshold for contraction); pCa_{50}, $[Ca^{2+}]$ required for half maximal activation (Ca^{2+} sensitivity); n_{Ca}, Hill coefficient for activation with Ca^{2+}, indicating the steepness of the force–pCa relationship; pSr_{10}, $[Sr^{2+}]$ required for 10% maximal activation (threshold for contraction); pSr_{50}, $[Sr^{2+}]$ required for half maximal activation (Sr^{2+} sensitivity); n_{Sr}, Hill coefficient for activation with Sr^{2+}, indicating the steepness of the force–pSr relationship. *$P < 0.05$ *versus* uninjured muscle fibres. Data based on muscles sampled from six rats for each of the time points 7, 14 and 21 days post-injury, including uninjured (control) muscles from the contralateral limb.

muscles were 10% of the cross-sectional area of muscle fibres from uninjured soleus muscles, and generated P_o values that were ∼12% that of uninjured soleus muscle fibre values (Table 2). These 7 d soleus muscle fibres were slightly more sensitive to Ca^{2+} compared with fibres from uninjured muscles (Fig. 2*B* and Table 2) but in contrast to 7 d EDL fibres, the 7 d soleus fibres exhibited a reduced sensitivity to Sr^{2+} compared with uninjured soleus muscle fibres (pSr_{50}; uninjured soleus 5.99 ± 0.01 *versus* 7 d soleus 5.49 ± 0.06, $P < 0.05$). This was also reflected in the nearly threefold greater $pCa_{50} - pSr_{50}$ values for typical 7 d soleus fibres compared with uninjured soleus muscle fibres ($pCa_{50} - pSr_{50}$; uninjured soleus, 0.26 ± 0.02 *versus* 7 d soleus 0.83 ± 0.06, $P < 0.05$, Table 2), although these were approaching control (uninjured) values by 14 d. The n_{Ca} and n_{Sr} values for 7 d soleus muscle fibres was increased ∼15–20% compared with uninjured soleus muscle fibres ($P < 0.05$, Table 2).

Fourteen days post-injury

At 14 days post-injury, fibres from regenerating EDL ($n = 21$) and soleus muscles ($n = 14$) remained ∼65% smaller than fibres from the respective uninjured muscles (Tables 1 and 2). Mean P_o of 14 d EDL and soleus muscle fibres was greater than that of 7 d fibres, but was still only 30% and 20% that of uninjured fibres, respectively (Tables 1 and 2). Regenerating EDL muscle fibres examined 14 days after injury maintained higher Ca^{2+} and Sr^{2+} sensitivities compared with uninjured fibres, and n_{Ca} values also remained lower ($P < 0.05$, Table 1). In contrast, the 14 d soleus fibres displayed Ca^{2+} and Sr^{2+} sensitivities that were similar to those of uninjured soleus muscle fibres but still had increased n_{Ca} values as for the 7 d soleus muscle fibres (Table 2). At 14 days post-injury, $pCa_{50} - pSr_{50}$ values remained lower in EDL muscle fibres and higher in soleus muscle fibres, respectively, compared with fibres from the uninjured EDL and soleus muscles (Table 2).

Twenty-one days post-injury

At 21 days post-injury (the last time point examined), regenerating EDL ($n = 17$) and soleus ($n = 19$) muscle fibres remained considerably smaller than respective uninjured fibres (Tables 1 and 2). P_o of 21 d EDL and soleus fibres was ∼45% and ∼36% of values for uninjured fibres from the respective muscles (Tables 1 and 2). Although 21 d EDL muscle fibres had a greater sensitivity to Ca^{2+} and Sr^{2+} than uninjured EDL muscle fibres, the differences between injured and uninjured fibres were less than those observed at either 7 or 14 days post-injury indicating a progressive development of contractile characteristics consistent with the mature fibre phenotype (Fig. 2*A*). This

observation was supported by the $pCa_{50} - pSr_{50}$ values for 21 d EDL muscle fibres which were not different from those of uninjured EDL muscle fibres (Table 1). The pattern of progressive change in the contractile characteristics of regenerating soleus muscle fibres was less evident since fibres examined at 21 days post-injury displayed similar Ca^{2+} sensitivities to fibres from control (uninjured) soleus muscles, but lower Sr^{2+} sensitivities compared with fibres examined at 14 days (Table 2). The 21 d soleus muscle fibres had ∼12% higher n_{Ca} values than uninjured soleus fibres, but similar n_{Sr} values (Table 2).

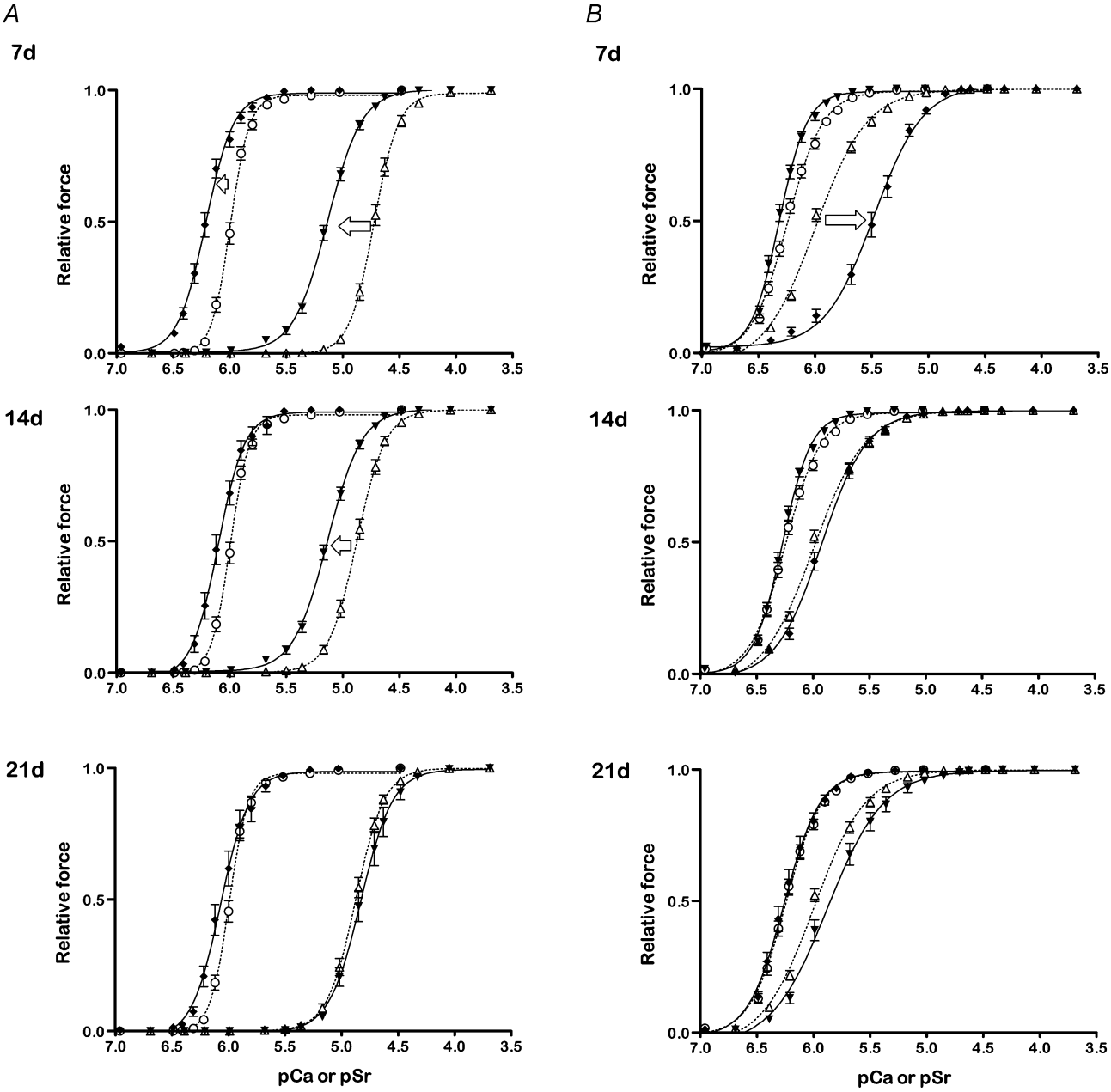

Figure 2. Force–pCa and force–pSr relations for permeabilized muscle fibres from uninjured and regenerating muscles

Force–pCa and force–pSr relations for permeabilized muscle fibres from uninjured (dashed lines) and regenerating EDL (*A*) and soleus (*B*) limb muscles (continuous lines) examined 7, 14 and 21 days post-injury. The symbols represent actual data points (means ± S.E.M.) and the curves represent the lines of best fit (see Methods). Arrows indicate the general shift in force–pCa (filled symbols) and force–pSr relations (open symbols) from the uninjured state during the time course of regeneration. The numbers of fibres in each case are those described in Tables 1 and 2 for each time point.

Table 2. Summary of data for permeabilized muscle fibres from uninjured and regenerating rat soleus muscles examined 7, 14 and 21 days after myotoxic injury

	Control ($n = 31$)	7 d ($n = 22$)	14 d ($n = 14$)	21 d ($n = 19$)
CSA (μm^2)	3480 ± 283	315 ± 40*	1132 ± 148*	1052 ± 121*
P_o (mN)	0.66 ± 0.04	0.07 ± 0.01*	0.16 ± 0.01*	0.24 ± 0.02*
sP_o (kN m^{-2})	207 ± 13	274 ± 26*	175 ± 24	276 ± 39*
pCa_{10}	6.54 ± 0.03	6.59 ± 0.03	6.54 ± 0.02	6.49 ± 0.04
pCa_{50}	6.25 ± 0.02	6.32 ± 0.02*	6.27 ± 0.01	6.23 ± 0.04
n_{Ca}	3.14 ± 0.11	3.77 ± 0.22*	3.54 ± 0.10*	3.53 ± 0.11
pSr_{10}	6.39 ± 0.02	6.00 ± 0.09*	6.32 ± 0.03	6.27 ± 0.05*
pSr_{50}	5.99 ± 0.01	5.49 ± 0.06*	5.92 ± 0.03	5.84 ± 0.05*
n_{Sr}	2.15 ± 0.06	2.43 ± 0.02*	2.31 ± 0.12	2.20 ± 0.13
$pCa_{50} - pSr_{50}$	0.26 ± 0.02	0.83 ± 0.06*	0.35 ± 0.03*	0.39 ± 0.05*

Values are means ± S.E.M.; *n*, no. of fibres. Refer to Table 1 for details.

Analysis of MyHC isoforms in regenerating muscle fibres

An example of the MyHC isoform composition in homogenates of uninjured and regenerating muscles at 7 days following myotoxic injury is presented in Fig. 3*A*. Although these data were obtained from homogenates of intact muscles rather than individual fibres, the information is useful in providing a better overview of the changes that are occurring in the muscle fibres. The uninjured EDL muscle was composed almost entirely (> 90%) of mature type II isoforms, while the soleus muscle was composed predominantly (∼60%) of the mature type I isoform.

In some instances, the IIa and IIx MyHC isoforms could not be separated and were thus combined and termed 'IIa–x' for all analyses. MyHC isoform composition was altered in regenerating EDL and soleus muscle (homogenates) compared with the respective uninjured muscles. Regenerating EDL muscles examined at 7 days post-injury contained a greater proportion of the neonatal MyHC isoform (∼45%) and a concomitant reduction in the proportion of IIa–x and IIb isoforms (Fig. 3*B*). Regenerating soleus muscles examined at 7 days had greater proportions of embryonic and neonatal MyHC isoforms (nearly 30% and 20% of the total, respectively) and considerably less mature type I MyHC isoform (Fig. 3*C*). Despite regenerating EDL and soleus muscles displaying markedly altered MyHC isoform distribution at 7 days post-injury compared with their respective uninjured muscles, the regeneration profile of the EDL and soleus muscles at this time, was still discernibly different.

By 14 days post-injury, regenerating EDL muscles displayed similar MyHC isoform composition compared with uninjured muscles, with the exception of some continued expression (∼5%) of the neonatal MyHC isoform (Fig. 3*B*). Regenerating EDL muscles examined at 21 days comprised MyHC isoforms in proportions that were indistinguishable from those of uninjured EDL muscles. Similar to regenerating EDL muscles, the regenerating soleus muscles examined at 14 days post-injury exhibited a pattern of MyHC isoform distribution more consistent with that of uninjured muscles, than 7 d soleus samples, but retained some expression of embryonic and neonatal isoforms (∼6% and 13%, respectively, Fig. 3*C*). MyHC isoform composition in 21 d regenerating soleus muscles was not different from that of uninjured soleus muscles.

Discussion

It is well established that skeletal muscles experience a loss of function following fibre injury, and that functional capacity is restored progressively in accordance with the full regeneration of replacement muscle fibres. However, the contractile activation characteristics of individual regenerating muscle fibres have not been studied extensively. We have shown that during early regeneration individual muscle fibres of innervated, vasculature-intact, regenerating fast-twitch EDL and slow-twitch soleus muscles of the rat exhibit activation characteristics significantly different from uninjured muscle fibres; that the contractile characteristics of fibres from fast and slow muscles are remarkably similar during the early stages of functional repair; and that the adoption of characteristics of typical mature fibres occurs earlier in fast than slow regenerating muscle fibres.

At 7 days post-injury, Ca^{2+} and Sr^{2+} sensitivities of regenerating EDL muscle fibres were greatly enhanced, but remarkably these had returned to control (uninjured) values by 21 days post-injury. Thus, although the force−pCa (−pSr) relationships for regenerating EDL

muscle fibres are initially shifted to higher sensitivity at 7 days compared with control, by 21 days these relationships are similar to those for control (uninjured) fibres, with only subtle differences in their activation characteristics (e.g. lower n_{Ca} and n_{Sr} values) persisting. At 7 days post-injury, Ca^{2+} and Sr^{2+} sensitivities of regenerating soleus muscle fibres were also greatly enhanced. However, unlike regenerating EDL muscle fibres, which showed a return to control values by 21 d post-injury, the force–pCa (–pSr) relationships remained different from those of control (uninjured) fibres. This was highlighted by the relative sensitivity to the activating ions ($pCa_{50} - pSr_{50}$) of regenerating soleus muscle fibres still being significantly different 21 days post-injury. Of particular interest was the similarity in the force–pSr characteristics of regenerating EDL and soleus muscle fibres at 7 days post-injury. This indicates that (at least) with respect to Sr^{2+} activation characteristics, the regenerating fibres appear to be starting from a common point and the possibility exists that the proteins regulating Sr^{2+} sensitivity are relatively homogeneous during the early stages of fibre regeneration. Overall, these findings would suggest that there are remarkable similarities between regenerating EDL and soleus muscle fibres in the earliest stages of recovery post-injury, and that their contractile characteristics develop increasingly disparate and specialized function as the muscle fibres mature.

The concept of there being heterogeneous sources of satellite cells in fast and slow muscles such as the EDL and soleus is substantiated by evidence *in vitro* where satellite cells isolated and cultured from regenerating muscles produce myotubes of eventually differing contractile and regulatory protein isoform composition, which 'characterize the donor myoblasts' even in the absence of the neural and mechanical influences of the *in vivo* environment (Feldman & Stockdale, 1991; Cantini *et al.* 1993; Rosenblatt *et al.* 1996). These differences may stem from subtle differences in the myogenic programme between populations of satellite cells, resulting in an inherent programming of satellite cells towards specific phenotypic development during regeneration (Martelly *et al.* 2000). This concept suggests an underlying predisposition towards fibre phenotype that is independent of neural, vascular and mechanical stimuli *in vivo*.

Isolated muscle fibres examined 7 days post-injury in the rat may be among the earliest developmental examples of those where function can be measured reliably since histological examinations indicate that structurally continuous rodent myotubes do not form *in vivo* earlier than 4–5 days after injury (Hurme & Kalimo, 1992; Picquet *et al.* 1997). Clearly, the regenerating muscle fibres are dramatically reduced in size (cross-sectional area) and their absolute force generating capacity at the earliest (7 d) time point examined was only ~10% that of

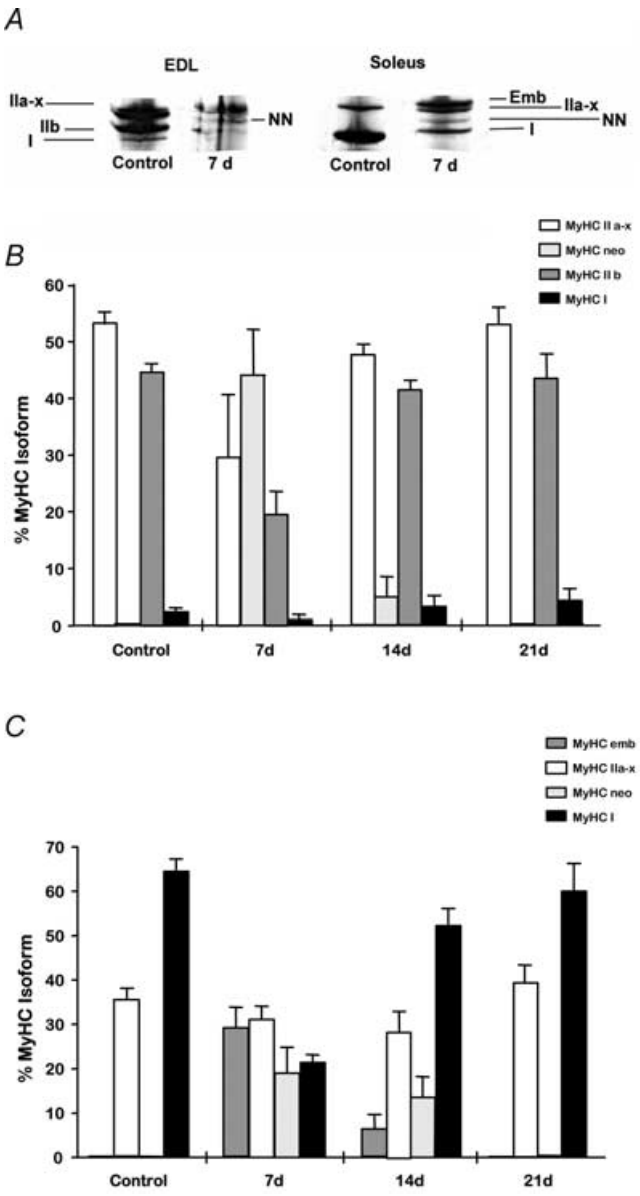

Figure 3. MHC isoform composition of uninjured and regenerating muscles

A, electrophoretic separation of myosin heavy chain (MyHC) isoforms in homogenates prepared from control (uninjured) and regenerating (7 days post-injury) EDL and soleus muscles. Note decreased type IIb MyHC in regenerating EDL muscle compared with control (uninjured) EDL muscle, and increased type II MyHC isoform expression in regenerating soleus muscles compared with control (uninjured) muscles. *B* and *C*, MyHC isoform composition of uninjured and regenerating EDL (*B*) and soleus (*C*) muscles examined at 7, 14 and 21 days post-injury. Analysis is based on densitometric evaluation of polyacrylamide gel electrophoretic separation of MyHC isoforms from muscle.

control (uninjured) fibres. It should be noted that even at 21 days post-injury when the force–pCa (–pSr) relations of regenerating muscle fibres are becoming similar to those for uninjured fibres, their absolute force producing capacity is still greatly reduced, but their specific force (absolute force normalized to fibre cross-sectional area) was not significantly different from control values.

The contractile apparatus of the skeletal muscle fibre is an elegant arrangement of many proteins that determine contractile performance (Reiser *et al.* 1988; Bortolotto *et al.* 2000; Bottinelli, 2001; Szczesna *et al.* 2002). Many studies have shown that the Ca^{2+} (and Sr^{2+}) activation characteristics of fast and slow fibres are determined by the expression of either slow (cardiac) or fast isoforms of troponin C (Hoar *et al.* 1988; Metzger *et al.* 1993; McDonald *et al.* 1995). Recent studies have also shown a close association between myosin heavy chain and troponin C isoform composition in skeletal muscle fibres of adult rats, highlighting the strong functional interplay between these proteins (O'Connell *et al.* 2004). Based on the extensive knowledge regarding the variations in functional protein isoform composition in regenerating skeletal muscles under various conditions, we sought to examine the contractile properties of regenerating muscle fibres using a model of regeneration not complicated by extensive neural or vascular disruption. The advantage of utilizing single fibre preparations is that assessment of function is based on the overall characteristics of the contractile apparatus and regulatory system and thus it is a highly sensitive preparation for revealing not only coarse but also subtle functional differences between muscle fibres. We have demonstrated that despite the myriad of neural, hormonal and mechanical stimuli that contribute to the definition of the phenotype of regenerating muscle fibres, there are remarkable similarities in the contractile activation characteristics between fast and slow fibres during early regeneration. In a model of injury–regeneration where nerves and vasculature are essentially preserved, the contractile activation characteristics of regenerating fast and slow fibres begin to assume their mature identity after 7 days, but it is important to note that not all functional properties are restored until 21 days or later.

Our findings are also interesting in the context of previous studies that have examined the Ca^{2+} and Sr^{2+} activation characteristics of muscle fibres from rats during different stages of normal postnatal development (Picquet *et al.* 1997) and from fetal and neonatal sheep (West *et al.* 1999). The latter study reported the paradoxical situation whereby at early stages of muscle development in sheep, the fast muscles have contraction dynamics of slow muscle but the slow muscle have activation profiles more characteristic of fast muscles (West *et al.* 1999). From postnatal days 6–17, soleus muscle fibres of rats exhibited Ca^{2+}- and Sr^{2+}-activated contractile characteristics that were intermediate between typical slow-twitch and fast-twitch properties, but by day 23 the activation characteristics of the soleus muscle fibres were closer to those of a slow type (Picquet *et al.* 1997). Our findings indicate remarkable similarities in the contractile characteristics of injured/early regenerating muscle fibres with those observed from muscle fibres sampled during the early stages of normal development (Picquet *et al.* 1997; West *et al.* 1999).

Although isolating and evaluating the functional performance of small regenerating muscle fibres from rodent muscles is technically challenging, our exciting findings advocate further examination of this model in order to understand the events controlling functional muscle regeneration. This would include comparative evaluation of regenerating fast and slow fibre function over the physiological range of motion (Reiser *et al.* 1988; Lynch & Faulkner, 1998), and an understanding of the events controlling excitation–contraction coupling in regenerating muscle fibres (Plant & Lynch, 2002, 2003). Further studies examining functional muscle regeneration would also include complementary analyses of contractile and regulatory protein isoforms during each of the different stages of functional cellular repair after injury.

References

Bigard XA, Janmot C, Merino D, Lienhard F, Guezennec YC & d'Albis A (1996). Endurance training affects myosin heavy chain phenotype in regenerating fast-twitch muscle. *J Appl Physiol* **81**, 2658–2665.

Bigard AX, Zoll J, Ribera F, Mateo P, Sanchez H, Serrurier B & Ventura-Clapier R (2001). Influence of overload on phenotypic remodeling in regenerated skeletal muscle. *Am J Physiol* **281**, C1686–C1694.

Bortolotto SK, Cellini M, Stephenson DG & Stephenson GM (2000). MHC isoform composition and Ca^{2+}- or Sr^{2+}-activation properties of rat skeletal muscle fibers. *Am J Physiol* **279**, C1564–C1577.

Bottinelli R (2001). Functional heterogeneity of mammalian single muscle fibres: do myosin isoforms tell the whole story? *Pflugers Arch* **443**, 6–17.

Bottinelli R & Reggiani C (2000). Human skeletal muscle fibres: molecular and functional diversity. *Prog Biophys Mol Biol* **73**, 195–262.

Cantini M, Fiorini E, Catani C & Carraro U (1993). Differential expression of adult type MHC in satellite cell cultures from regenerating fast and slow rat muscles. *Cell Biol Int* **17**, 979–983.

Carlson BM, Dedkov EI, Borisov AB & Faulkner JA (2001). Skeletal muscle regeneration in very old rats. *J Gerontol* **56A**, B224–B233.

Carlson BM & Faulkner JA (1983). The regeneration of skeletal muscle fibers following injury: a review. *Med Sci Sports Exerc* **15**, 187–198.

Carlson BM & Faulkner JA (1996). The regeneration of noninnervated muscle grafts and marcaine-treated muscles in young and old rats. *J Gerontol* **51A**, B43–B49.

d'Albis A, Couteaux R, Janmot C, Roulet A & Mira JC (1988). Regeneration after cardiotoxin injury of innervated and denervated slow and fast muscles of mammals. Myosin isoform analysis. *Euro J Biochem* **174**, 103–110.

Devor ST & Faulkner JA (1999). Regeneration of new fibers in muscles of old rats reduces contraction-induced injury. *J Appl Physiol* **87**, 750–756.

Donovan CM & Faulkner JA (1987). Plasticity of skeletal muscle: regenerating fibers adapt more rapidly than surviving fibers. *J Appl Physiol* **62**, 2507–2511.

Erzen I, Primc M, Janmot C, Cvetko E, Sketelj J & d'Albis A (1999). Myosin heavy chain profiles in regenerated fast and slow muscles innervated by the same motor nerve become nearly identical. *Histochem J* **31**, 277–283.

Feldman JL & Stockdale FE (1991). Skeletal muscle satellite cell diversity: satellite cells form fibers of different types in cell culture. *Dev Biol* **143**, 320–334.

Fink E, Fortin D, Serrurier B, Ventura-Clapier R & Bigard AX (2004). Recovery of contractile and metabolic phenotypes in regenerating slow muscle after notexin-induced or crush injury. *J Muscle Res Cell Motil* **24**, 421–429.

Fink RH, Stephenson DG & Williams DA (1986). Potassium and ionic strength effects on the isometric force of skinned twitch muscle fibres of the rat and toad. *J Physiol* **370**, 317–337.

Gregorevic P, Williams DA & Lynch GS (2002). Periodic hyperbaric oxygen exposure enhances contractile function of the regenerating rat soleus muscle following myotoxic injury. *Med Sci Sports Exer* **34**, 630–636.

Hoar PE, Potter JD & Kerrick WG (1988). Skinned ventricular fibres: troponin C extraction is species-dependent and its replacement with skeletal troponin C changes Sr^{2+} activation properties. *J Muscle Res Cell Motil* **9**, 165–173.

Hurme T & Kalimo H (1992). Activation of myogenic precursor cells after muscle injury. *Med Sci Sports Exer* **24**, 197–205.

Hurme T, Kalimo H, Lehto M & Jarvinen MSO (1991). Healing of skeletal muscle injury: an ultrastructural and immunohistochemical study. *Med Sci Sports Exer* **23**, 801–810.

Lamb GD & Posterino GS (2003). Effects of oxidation and reduction on contractile function in skeletal muscle fibres of the rat. *J Physiol* **546**, 149–163.

Lynch GS & Faulkner JA (1998). Contraction-induced injury to single muscle fibers: velocity of stretch does not influence the force deficit. *Am J Physiol* **275**, C1548–C1554.

Lynch GS, Stephenson DG & Williams DA (1995). Analysis of Ca^{2+} and Sr^{2+} activation characteristics in skinned muscle fibre preparations with different proportions of myofibrillar isoforms. *J Muscle Res Cell Motil* **16**, 65–78.

Marechal G, Schwartz K, Beckers-Bleukx G & Ghins E (1984). Isozymes of myosin in growing and regenerating rat muscles. *Euro J Biochem* **138**, 421–428.

Martelly I, Soulet L, Bonnavaud S, Cebrian J, Gautron J & Barritault D (2000). Differential expression of FGF receptors and of myogenic regulatory factors in primary cultures of satellite cells originating from fast (EDL) and slow (Soleus) twitch rat muscles. *Cell Mol Biol* **46**, 1239–1248.

McDonald KS, Field LJ, Parmacek MS, Soonpaa M, Leiden JM & Moss RL (1995). Length dependence of Ca^{2+} sensitivity of tension in mouse cardiac myocytes expressing skeletal troponin C. *J Physiol* **483**, 131–139.

Metzger JM, Parmacek MS, Barr E, Pasyk K, Lin WI, Cochrane KL, Field LJ & Leiden JM (1993). Skeletal troponin C reduces contractile sensitivity to acidosis in cardiac myocytes from transgenic mice. *Proc Natl Acad Sci U S A* **90**, 9036–9040.

Moisescu DG & Thieleczek R (1978). Calcium and strontium concentration changes within skinned muscle preparations following a change in the external bathing solution. *J Physiol* **275**, 241–262.

Noirez P, Agbulut O & Ferry A (2000). Differential modification of myosin heavy chain expression by tenotomy in regenerating fast and slow muscles of the rat. *Exp Physiol* **85**, 187–191.

Noonan TJ, Best TM, Seaber AV & Garrett WE (1994). Identification of a threshold for skeletal muscle injury. *Am J Sports Med* **22**, 257–261.

O'Connell B, Nguyen LT & Stephenson GMM (2004). A single-fibre study of the relationship between MHC and TnC isoform composition in rat skeletal muscle. *Biochem J* **378**, 269–274.

Pette D, Sketelj J, Škorjanc D, Leisner E, Traub I & Bajrovic F (2002). Partial fast-to-slow conversion of regenerating rat fast-twitch muscle by chronic low-frequency stimulation. *J Muscle Res Cell Motil* **23**, 215–221.

Pette D & Staron RS (2000). Myosin isoforms, muscle fiber types, and transitions. *Microsc Res Tech* **50**, 500–509.

Picquet F, Stevens L, Butler-Browne GS & Mounier Y (1997). Contractile properties and myosin heavy chain composition of newborn rat soleus muscles at different stages of postnatal development. *J Muscle Res Cell Motil* **18**, 71–79.

Plant DR & Lynch GS (2001). Rigor force responses of permeabilized fibres from fast and slow skeletal muscles of aged rats. *Clin Exp Pharm Physiol* **28**, 779–781.

Plant DR & Lynch GS (2002). Excitation–contraction coupling and sarcoplasmic reticulum function in mechanically skinned fibres from fast skeletal muscles of aged mice. *J Physiol* **543**, 169–176.

Plant DR & Lynch GS (2003). Depolarization-induced contraction and SR function in mechanically skinned muscle fibers from dystrophic mdx mice. *Am J Physiol* **285**, C522–C528.

Reiser PJ, Kasper CE, Greaser ML & Moss RL (1988). Functional significance of myosin transitions in single fibers of developing soleus muscle. *Am J Physiol* **254**, C605–C613.

Rosenblatt JD (1992). A time course study of the isometric contractile properties of rat extensor digitorum longus muscle injected with bupivacaine. *Comp Biochem Physiol* **101A**, 361–367.

Rosenblatt JD, Parry DJ & Partridge TA (1996). Phenotype of adult mouse muscle myoblasts reflects their fiber type of origin. *Differentiation* **60**, 39–45.

Rosenblatt JD & Woods RI (1992). Hypertrophy of rat extensor digitorum longus muscle injected with bupivacaine. A sequential histochemical, immunohistochemical, histological and morphometric study. *J Anat* **181**, 11–27.

Snoj-Cvetko E, Sketelj J, Dolenc I, Obreza S, Janmot C, d'Albis A & Eržen I (1996). Regenerated rat fast muscle transplanted to the slow muscle bed and innervated by the slow nerve, exhibits an identical myosin heavy chain repertoire to that of the slow muscle. *Histochem Cell Biol* **106**, 473–479.

Stephenson DG & Williams DA (1982). Effects of sarcomere length on the force-pCa relation in fast- and slow-twitch skinned muscle fibres from the rat. *J Physiol* **333**, 637–653.

Szczesna D, Zhao J, Jones M, Zhi G, Stull J & Potter JD (2002). Phosphorylation of the regulatory light chains of myosin affects Ca^{2+} sensitivity of skeletal muscle contraction. *J Appl Physiol* **92**, 1661–1670.

Talmadge RJ & Roy RR (1993). Electrophoretic separation of rat skeletal muscle myosin heavy-chain isoforms. *J Appl Physiol* **75**, 2337–2340.

West JM, Barclay CJ, Luff AR & Walker DW (1999). Developmental changes in the activation properties and ultrastructure of fast- and slow-twitch muscles from fetal sheep. *J Muscle Res Cell Motil* **20**, 249–264.

Whalen RG, Harris JB, Butler-Browne GS & Sesodia S (1990). Expression of myosin isoforms during notexin-induced regeneration of rat soleus muscles. *Dev Biol* **141**, 24–40.

Acknowledgements

Supported by research grants from the Muscular Dystrophy Association (USA) and the Australian Research Council (ARC).